Method for Significantly Increasing Computational Speed, Accuracy and Versatility of Electromagn tic Reconstruction of Shapes and Composition of Compl x Targets Containing Lossy Materials

Inventors: Eytan Barouch (Brookline, MA), Stephen L. Knodle (Newton,MA)
Assigned to EMIT Systems Co.

Cross Reference to Related Applications

Benefit is claimed, under 35 U.S.C. =A7 119(e)(1), to the filing date of provisional patents applications serial numbers 60/420,090 and 60/419,834 , entitled "Method for analyzing light simultaneously of all wavelengths scattered off 2D or 3D micro- or nano-electronic structures", and "Method for significantly reducing the oscillatory nature of scattered polarized radiation to better enable the solution of the inverse problem of determining the properties of the scatterer", both filed on 10/21/2002 and both are listing Eytan Barouch, Brookline MA; as inventor, for any inventions disclosed in the manner provided by 35 U.S.C. A7 112, B6 1. These provisional applications are expressly incorporated herein by reference.

Field of the Invention

The thrust of this invention is a new methodology for very fast and accurate of structure and composition of objects at wide range of sizes, scattering a wide band of electro-magnetic radiation. This invention includes analytical, algorithmic and practical numerical implementation by analyzing the reflected light off of micro- and nano-electronics features for advanced metrology applications, thereby enabling the sizes and features of the structures to be determined on location in real time in a manufacturing environment.

Background of the Invention

This patent application has to do with a method and algorithm that can be used in conjunction with scatterometry apparatus. The following background, quoted from the background of US patent #5,963,329, serves fairly well here also as a starting point on the optical measurement of micro and nanoelectronic structures:

"In microelectronics, accurate measurement of feature profiles (i.e. line width, line height, space between lines, and sidewall shape) are very important to optimizing device performance and chip yield. Measurements are needed at many steps in manufacturing to assure that critical dimensions, line profiles, and feature depths are under control. Historically, measurements have been accomplished with the following technologies:

Optical imaging using the resolving power of optical microscopes and image processing to measure small f atur s. Howev r, f atures smaller than the resolving power of the microscop can not be measur d, nor can the line profile.

Electron-beam imaging, particularly th scanning electron microscope (SEM), greatly improves resolution ov r the optical microscop . However, like optical imaging, top-down SEM imaging d es not provide profile information. Whil imaging a cross-s ctioned sampl s d es provid profil information, cross s ctioning is d structiv , costly, and labor intensiv . In addition the signal processing us d in SEM imaging introduces uncertainties. Furth rmore, electron beams can damage the sample, and this is especially th cas when sensitive materials such as photoresist are imaged. In addition, electron beam charging can seriously distort measurement signals, causing beam position deviations. To overcome this problem, conductive coatings are commonly used but coatings or their removal can damag the sample or effect measurement accuracy.

Scanning force microscopy (SFM) utilizes a very small mechanical probe to sense minute atomic forces that act very close to the surface of materials, and SFM can provide high-resolution topographical information, including line profiles. Unfortunately, SFM is slow and operator-intensive, and the quantitative science of the probe tip is uncertain and unreliable.

Surface-contact mechanical-probe technologies, such as surface profilometers, have been used to profile large structures but do not offer the resolution or sensitivity required by today's characterization requirements. Furthermore, contact-probes distort surfaces. In addition, mechanical stability requirements prohibit the use of probes small enough to accommodate the sub micrometer sizes commonly measured. To measure the width of a lin the location of each edge of its profile must be defined, and an arbitrary, qualitative edge detection model is usually used in each of the above measuring techniques. While this arbitrary measurement point is typically calibrated to a cross-section, manufacturing process changes and normal manufacturing process drift can invalidate the edge model and introduce significant measurement error.

Furthermore, none of the above techniques can characterize planarized, buried sub-micron structures that commonly are found in microelectronic or micro-machining manufacturing processes. Features may be formed that are later covered with a transparent (or semi-transparent) layer of material, which is then planarized. If the feature sizes are below the resolution limits of optical techniques and the flat top surface prevents SEM and AFM imaging, none of the above well-known techniques will work.

Two optical techniques are available for planarized buried structures. Scatterometry has been used for characterizing periodic topographic structures in which a light beam (typically a laser) illuminates an area to be characterized and the angular distribution of elastically scattered light is used to measure line widths on photomask and silicon wafer gratings. However, scatterometry requires a high degree of mechanical stability and accurate measurement of the laser beam impingement angle on the grating, and these mechanical limitations contribute to the uncertainty of scatterometry results.

Confocal laser imaging is another optical technique that permits characterization of planarized buried structures. Focus on the sample is progressively adjusted with a monochromatic, high numerical aperture (NA) optical imaging system, and those focus adjustments provide the line profile. The high NA lens has a very small depth of focus, and therefore, a physical profile can be obtained by moving through a series of focus settings up or down the features, and recording those height variations. However, the technique is limited by the resolution of the laser beam, or the size f the las r spot on the sampl . Furthermore, the us of a high NA objectiv lens, providing a large angl to the incid nt beam limits the ability to characteriz high aspect ratio features that ar commonly found in semiconductor manufacturing."

Patent numb r 5,963,329 went a long way toward improving the above situation. As quot d in the summary of that pat nt:

"It is th r fore an obj ct of the pr sent invention to provid an optical method of d termining a line profile of a sub-micron structure. It is a f ature of th pres nt inv ntion that the line profile is determined by comparing measured diffraction radiation intensity from a periodic structure on a substrate with modeled radiation intensity predicted from a theoretical line profile. It is a feature of the present invention that line profile parameters of the model are varied until the predicted intensity converges to the measured intensity. It is a feature of the present invention that a rigorous and detailed two-dimensional analytical solution is obtained for the line profile. It is an advantage of the present invention that the line profile is reliably, reproducibly, rapidly, and nondestructively, obtained. These and other objects, features, and advantages of the invention are accomplished by a method of determining the profile of a line comprising the steps of: (a) providing a substrate having a repeating structure comprising a plurality of lines, said lines having substantially identical profiles; (b) illuminating said repeating structure with radiation wherein said radiation diffracts, said diffracted radiation having an intensity; (c) measuring said intensity; (d) providing a model structure on a data processing machine, said model structure comprising a repeating structure on said substrate, said model structure comprising a model profile; ( ) mathematically predicting a predicted diffracted radiation intensity when said model structure is illuminated with said radiation; and (f) comparing said predicted intensity with said measured intensity."

The present invention has to do with an advanced algorithm that works well with either scatterometry or ellipsometry equipment, but in particular shows its highest advantage when used with analyzing light gathered in the usual method of scatterometry.

Now, there is another class of measurement technology, namely, ellipsometry, that we need to mention here that does involve the measurement of light reflected off of substrates at an angle, and measuring the change in intensity and polarization. By describing some of the operation of this measurement procedure, some of the aims/purposes of the present invention will become clearer. In a conventional ellipsometry set-up, the angle of incidence and the angle of reflection of the beam, to the normal of the substrate, are made as nearly equal to each other as possible. Ellipsometry is well known for being able to deduce the complex index of refraction of the substrate, for each wavelength of light used in the illumination. More specifically, by shining well collimated light, at some angle to the normal, of a substrate material, and by collecting and measuring the intensity of the reflected light at the same angle to the normal, and by determining the change in polarization, then it is well known that one can deduce what the complex index of refraction, $\check{n}(\omega)=n(\omega)+ik(\omega)$ will be, for each wavelength of light for which this measurement is made. If the substrate has a singl , uniformly composed film layer on it, and if one knows the substrate's optical properties [e.g., $\check{n}(k)$], and if the film is transparent, then the real part of the complex index of the film, and the film's thickness, can also be deduced. If one has a stack of films, then one can also determine the effective complex index of refraction of the stack of films, provided other information is supplied.

In general, in ellipsometry, the angle of incidence to the normal of the substrate, and the angl of r flection from the substrate, ar mad identical. For each stat of incident radiation (known wav length, known polarization state, and known angl of incid nce to the sample), two measurements can be mad , namely, th int nsity of th light scattered into the reflected beam, for each of two polarization stat s that can always be used to characterize th refl cted beam. Thus, there ar two measurements that can be mad for each incid nt

ray and polarization state onto the sample. In the case of a flat substrat , without structure and without films, then th se two measurements can be used to deduce *n* and *k* for th substrate. If a film exists on th substrate, th n *n* and *k* for the substrat , and *n* and *k* for the film, and the thickness *d*, cannot all be deduced, as one only has two piec s of information (change in int nsity of light into the reflected beam for ach exiting polarization state). However, by measuring the substrat properties first without the film, then supplying the information of *n* and *k* of the substrate in the second set of measurements of involving the film on the substrate, then one can reduce the number of unknowns in the composite system. There are still too many unknowns, however, namely, *n*, *k*, and *d* for the film. However, if the film is transparent, so that $k=0$, or if independently one can measure the absorption properties of the film, then one can use the two sets of data obtained from the ellipsometry measurement to deduce *n* and *d* for the film. Similar, but more complicated procedures, can be pursued to obtain information about stacks of uniform films [2].

In general ellipsometry practice, there are two other commonly used means for collecting yet more information about the planar substrate and composite film structure. The same set of measurements just described can be done carried out as a function of wavelength, by simply using a broadband light source and filtering the incident light to make it of a narrow wavelength, or quasi-monochromatic, character. For each incident light situation of distinct wavelength, one can carry out the same measurements just described. Thus, one can measure the change in intensity of each polarization state, for more than one wavelength of incident radiation, to thereby gain information regarding the complex index $\varepsilon(\omega)=n(\omega)-ik(\omega)$, where $n(\omega)$ and $k(\omega)$ are functions of the frequency ω. Furthermore, by carrying out this sam measurement scenario for different angles of incidence for the radiation on the substrate plane, then yet another entire multiplicity of measurements can be obtained. Thus, for each angle of incidence of light, and for each wavelength of light used in the illumination, ther are two measurements that can be obtained in the beam of reflected light, where the reflected light angle to the normal, in ellipsometry, is made equal to the incident angle of the directed light. Most of these points will have bearing on the invention to be described her . Thus, ellipsometry has to do with measuring the properties of light reflected off at an angle from a substrate, with possible layers of uniform film on the substrate, where the incident and reflected light beams have the same angle to the normal to the substrate. Scatterometry has to do with the detection of scattered radiation off of a substrate, typically with a periodic structure in or on the substrate, where one or more angles of scatter from the normal are examined, and where the intensity and polarization of the light, for each wavelength, are compared with that of the incident radiation.

As for the algorithm that is conventionally used in analyzing light obtained via scatterometry methods, the typical technique is to follow a rather computationally intensive approach involving optimizing the number and sizes of a large number of "slabs"of photoresist to yield a refl ctivity versus wavelength curve that most closely match the intensity data. Other researchers hav also made investigations in scatterometry along these lines, or via matching precalculated libraries of shapes. The present invention does not have any of these limitations.

Brief Summary of the Invention

In this invention we address these consideration in by developing a system of processes described in figure 1. The first task is to valuat th system being examined for g neral properties, type of mat rials involv d and their lectromagn tic prop rties. An important d cision is wh th r said materials contain some inh rent non-lin ar polarization properties. Th sizes of the featur s (nano, micro or much larger) as well as th rang of ne d d wavel ngths (or frequ ncies) to r solv and reconstruct the features is valuated at this initial st p. Next ar thre simultaneous steps: mat rial charact rization as a function of

frequency immediately transformed to time domain, a "rendering algorithm' characterizing the scattering object with its seed composition and shap and spatial computational m sh with its corr sponding time steps and stability and pr cisi n crit ria, so a cost function for xit can be defined. The next step consists of inserting th various mat rials and scattering objects into the dev loped very-fast and accurate forward scatt ring algorithm using hybrid method similar to multi-grid analysis, computing the TE, TM polarization of th reflect d waves and then the non-polarized spectrum, to go into the cost function for comparison against the target spectrum. Then the structure and composition are updated by various methods (like least square or conjugate gradient) to provide an updated composition and shape to be put back into the system iteratively. When the cost-tolerance is obtained, the system exits and reports its findings.

Statement Regarding Fed sponsored R&D

The invention reported in the current patent application has not been sponsored by any US Federal government agency.

List of Figures and Tables

Figures:

1. Invention organizational chart.
2. Figures 2,3,4 illustrate the powerful innovation embedded in the module "Findpoles". In said figures a comparison between target optical parameters and their computed permittivity function is demonstrated, with excellent agreement.
3. The result of "Findpoles" is applied to a current realistic stack of four layers and the computed and measured spectra are exhibited in figure 5, using the module "Fwd".
4. In figures 6,7,8,9 a photolithography state of the art system is displayed, comparing 300nm and 400nm pitches of lines and spaces (L/S). The industrially measured spectra under manufacturing conditions are employed as targets for the module "Invscat" and the closest agreement is given. The reconstructed feature agrees with the SEM measurements to about .4%.

Tables:

1. Table 1 shows the input format for the target of "Findpoles".
2. Table 2 shows the seed format for "Findpoles"
3. Table 3 shows the output format of "Findpoles".

Description of the Invention

This patent application involves a new methodology to solve Material-Maxwell's equations for electromagnetic scattered beam of composite lossy substrates and isolated or periodic complex and composite objects containing metals as well as absorbing lossy materials. As such, it allows the microchip industry to detect and evaluate critical dimension, affording determination of the manufacturability of micro and nanoelectronic structures. This method of analysis is equally valid for all wavelengths of interest and can be done simultaneously in r al tim on a singl proc ssor for transvers electric (TE) and for transverse magnetic (TM) polarizations. The Material-Maxwell's equations naturally d compos into two separate syst ms (TE and TM) that can b solved simultaneously. Earlier work as d scribed in US patents # 5,963,329, 6,433,878 addresses both facts that the range of validity is v ry limited and the versatility of shape r construction ability is limited to parallel layers only due to the

in fficiency of the RCWP th ory. Also, both are limit d to one wavelength sinc per calculation sinc they us an algorithm valid only in frequency spac . Another limiting applicability of the RCWP method is its complete disregard to fr quencies in the high and low domain, resulting in severe limitati ns at th de p UV (ultra-violet) range, where most current action takes plac .

In this invention we address these consideration in by developing a system of processes described in figure 1. The first task is to evaluate the system being examined for general properties, type of materials involved and their electromagnetic properties. An important decision is whether said materials contain some inherent non-linear polarization properties. The sizes of the features (nano, micro or much larger) as well as the range of needed wavelengths (or frequencies) to resolve and reconstruct the features are evaluated at this initial step. Next are three simultaneous steps: material characterization as a function of frequency immediately transformed to time domain, a "rendering algorithm' characterizing the scattering object with its seed composition and shape and spatial computational mesh with its corresponding time steps and stability and precision criteria, so a cost function for exit can be defined. The next step consists of inserting the various materials and scattering objects into the developed very-fast and accurate forward scattering algorithm using hybrid method similar to multi-grid analysis, computing the TE, TM polarization of the reflected waves and then the non-polarized spectrum, to go into the cost function for comparison against the target spectrum. Then the structure and composition are updated by various methods (like least square or conjugate gradient) to provide an updated composition and shape to be put back into the system iteratively. When the cost-tolerance is obtained, the system exits and reports its findings.

The most critical components of the invention are:

a. The material composition function is obtained by the use of the module "Findpoles". This module takes a seed table exhibited in Table 2 with the target table exhibited in Table 1. Table 2 expresses the seed as a sum of Debye, Lorenz, Lorenz, Conductivity, plasma and Constant terms. It is then converted to the format given in Table 1, whos columns are the energy in eV, n, k, real permitivity, imaginary permitivity, reflectance and wavelength in nm. A complicated least-square code "Findpoles" is turned on and when tolerance is obtained it exits with the output file displayed in Table 3. There, the inherent frequencies of the material are given in terms of 1/sec, as well as the relaxation parameters. The strength of each term is dimensionless and the conductivity is given in terms of Siemens. As a by product, "Findpoles" provides an efficient and useful extraction method of *n&k*, that satisfies causality restrictions unlike the claim in US patent # 4,905,170, where causality is violated, rendering it useless for electromagnetic calculations in time domain.
b. The speed of the forward scattering module "Fwd" is largely obtained due to the ability to express the very large domain of substrate material in terms of a very few grid grid-cells (~10). This innovation is achieved by a mathematical formulation depicting the large substrate layer as having a "slave" attached lossy layer with equal impedence of the substrate material, thus cutting down the most expensive part of the computational domain substantially, obtaining thousands-fold speed-up. The "slave" layer has poles of the *same* frequency as the substrate material with differ nt coefficients obtained from equalizing the impedances.
c. The reconstruction of th scattering object is performed with a hybrid method similar to th LM algorithm with one fundamental variation. Th initial Hessian is obtain d by localized paramet r minimizations, avoiding the xtreme inaccuracy involved with numerical derivativ s. The initially construct d Hessian provides both seed as well as vector-directions utilizing a Gram-Schmidt proc dure.

Figur s 2,3,4 illustrate the powerful innovation emb dded in the module "Findpoles". In said figur s a comparison betw n targ t optical paramet rs and their comput d permittivity function is demonstrated, with xcell nt agr ement. Th result of "Findpol s" is applied to a curr nt realistic stack of four layers and the computed and measured spectra are xhibited in figur 5, using the module "Fwd". In figur s 6,7,8,9 a photolithography stat of the art system is displayed, comparing 300nm and 400nm pitches of lines and spaces (L/S). The industrially measured spectra under manufacturing conditions are employed as targets for the module "Invscat" and the closest agreement is given. The reconstructed feature agre s with the SEM measurements to about .4%.

The method described in this invention is accomplished by providing a detailed analysis of the dielectric function of each material in the structure of interest. The functional form of the dielectric function can be expressed in one of two ways. First, it can be given as a sum of a constant and an interactive plasma term (non-magnetized) and several poles of Debye, Lorenz double poles and Linear-Lorenz double poles. Second, the dielectric function may be express d in terms of the density of states in the corresponding quantum mechanical band, as expressed in an integral equation of Cauchy type, i.e., with a singular kernel, that satisfies the fundamental Kramers-Kronig relationship and is solved by a combination of analytic and numerical techniques. An approximate analytic solution of the integral equation corresponds to a high level of accuracy to the first method just mentioned. The permitivity so described is a representation of the dielectric function in frequency space, and utilized as such forces solution of the Material-Maxwell equations for *each* wavelength separately, resulting in a very slow execution tim as well as severe inaccurate and unreliable results. Consequently, despite the patent of ref. 1, IBM has initially rejected this technology. Furthermore, the dielectric function in frequency spac must satisfy several strict restrictions in order for it to represent the real physics it attempting to describe. These restrictions include the Kramers-Kronig relations, causality, positivity of the index of refraction *n* and the absorption coefficient *k,* as well as the property that the complex conjugate of the permittivity function as a function of frequency ω is a function of $-\omega$. The real part of the permittivity function is allowed to be positive and negative continuously, presenting another usually ignored difficulty when the real part vanishes. When that happens all classical electromagnetic descriptions become invalid in frequency space and disregarding it for th frequency in which it takes place yields absurd results. A typical material in which this tak s place is Silicon, which is a critical material for the microchip industry. The physics behind this occurrence is a change in response of the material from semi-conductor to a temporary plasma containing material. This invention deals in part with overcoming this complication. The time domain dielectric function is the Fourier transform of the permittivity function in frequency spac , and as such it is not subjected to the separation of the real and imaginary parts. However, there is a high price to pay. The Material-Maxwell equations are no longer partial differential equations since they become integral-partial-differential (IPD) system, which is much harder to handl . An integral part of this invention is the incorporation of the properly characterized material functions into the IPD system allowing a very rapid evaluation of the forward scattering for all wavel ngths contained in the source, simultaneously.

For the microchip industry, the Material-Maxwell solver of this invention uses a few nanometer grids. However, the feature that designates the target needs to be characteriz d up to a fraction of a nanometer. Thus, a rendering algorithm has been developed that divid s each grid cell into an arbitrary localized refined mesh where the various weights on the original grid c lls are modified according to th materials includ d in that cell. For xampl , if each boundary cell is divided into a 10x10 grid, th CD accuracy thus obtained is 0.5 nm. This t chniqu , r cently developed and unpublish d, is mploy d to comput th inverse pr blem of determining the scatt ring object shape and material composition from the knowl dg of the incoming and the scatt red b ams. It also allows alignment d t rmination

of alignment markers and shapes. The speed and accuracy of th s algorithms would enabl *in-situ* and on-line metrology for realistic syst ms.

This invention is equally applicable to 2D&3D micro and nanoel ctronic structures. By th development of this method, insp ction of OPC (optical proximity corrections) can b btained in a manufacturing environm nt, while taking into account alignment and twist location structures.

Claims

What is claimed is:

1 A method of solving Material-Maxwell's equations for the analysis of light scattered off 2D or 3D micro or nanoelectronic structures, such that all wavelengths of the incident light can be analyzed and computed simultaneously in real time on a singl processor for transverse electric (TE) and for transverse magnetic (TM) polarizations.

2 A method as recited in claim 1, wherein said method is sufficiently general that it can be used on either single or multiple processors.

3 A method as recited in claim 1, wherein said method is applicable to microwave technology of range of a few cm wavelengths.

4 A method as recited in claim 1, wherein said method is able to process complicated lossy material structures, utilizing a unique method of analyzing very large domains in terms of a transformation of small finite domains.

5 A method as recited in claim 1, wherein said method is applied to microchip fabrication encompassing a range of 50nm-1500nm uniformly.

6 A method as recited in claim 1, wherein said method is comprising of a "rendering algorithm" that enables the use of a larger numerical grid than the smallest feature sizes, but that enables the scattering target to be characterized up to a fraction of this size.

7 A method as recited in claim 1, wherein said method is employed in the computation of reflected spectra for TE&TM polarization, reporting their ratio as a function of frequency, thus eliminating any spurious oscillations associated with the source.

8 A method of constructing an electrical susceptibility function in time-domain spac utilizing measurable optical constants. The components of said function are Lorenz poles, Xlorenz-linear poles, Debye poles, conductivity term, a non-magnetized plasma term and a limiting constant for infinite wavelength.

9 A method as recit d in claim 8, wh rein said method is satisfying strict causality properti s in time domain space.

10 A method as recited in claim 8, wherein said method guarante s that th refractiv index and the absorption coeffici nts (*n&k*) are positive for all wavelengths.

11 A m thod as recited in claim 8, wh rein said method allows extraction of said *n&k* recited in claim 10 satisfying strict causality r lations, term by term.

12 A method as recited in claim 8, wherein said method provides the structured boundary layer representing large or semi-infinite domain, with poles determined from recited susceptibility function of claim 8, with variation of the coefficients in the numerators, obtained by imposing a non-reflection condition. The conductivity term becomes a mixture of conductivity and collisionless plasma and the plasma term becomes a combination of cited conductivity and Debye terms.

13 A method of scattering object's complex shape and composition.

14 A method as recited in claim 13, wherein said method constructs a seed Hessian without employing numerical derivative, using local parameter minimization as a guide.

15 A method as recited in claim 13, wherein said method makes the reconstruction problem less ill posed by reducing the oscillatory nature of the scattered radiation, by eliminating the need to normalize the radiation source, and analyzing the ratio and relative phase of the TM and TE polarization for each wavelength of interest as the backbone of the cost function.

16 A method as recited in claim 13, wherein said method is equally valid for 2D and 3D structures.

References Cited:

US PATENT DOCUMENTS

4,905,170	02/27/1990	Forouhi *et. al.*
5,963,329	10/05/1999	Conard *et. al.*
6,433,878	10/14/2002	Niu *et. al.*

Other Publications

R. M. A. Azzam and N. M. Bahara, "Ellipsometry and Polarized Light," North-Holland, Amsterdam, 1987.

J. Allgair, D. C. Benoit, et. al, "Manufacturing considerations for implementation of scatterometry for process monitoring, metrology, inspection, and process control for microlithography" XIV, Proc. SPIE 3998, pp. 125-134, 2000.

X. Niu, N. Jakatdar, t. al, "Specular spectroscopic scatterom try," IEEE Trans. S miconductor Manufacturing, Vol. 14, No. 2, pp. 97-111, 2001.

H.T. Huang, W. Kong, and F. L. T rry, Jr., "Normal-incid nce spectroscopic ellipsom try for critical dimension monitoring," Appl. Phys. Lett., Vol. 78, No. 25, pp. 3983-3985, 2001.

Invention Organization

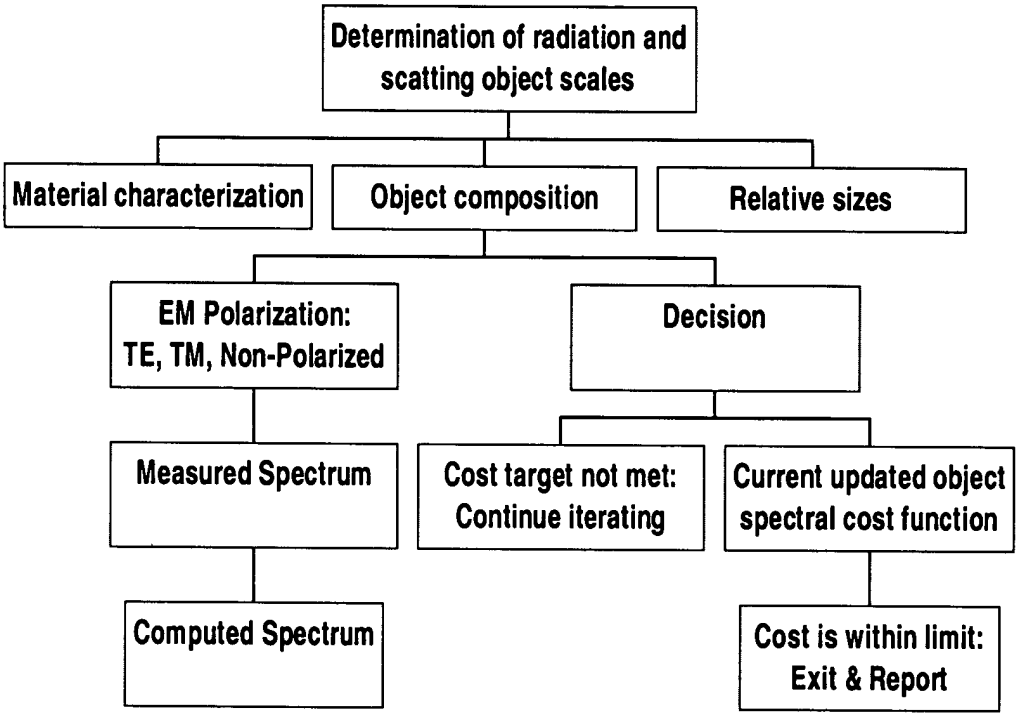

Figure 1: Organizational chart of the invention road map.

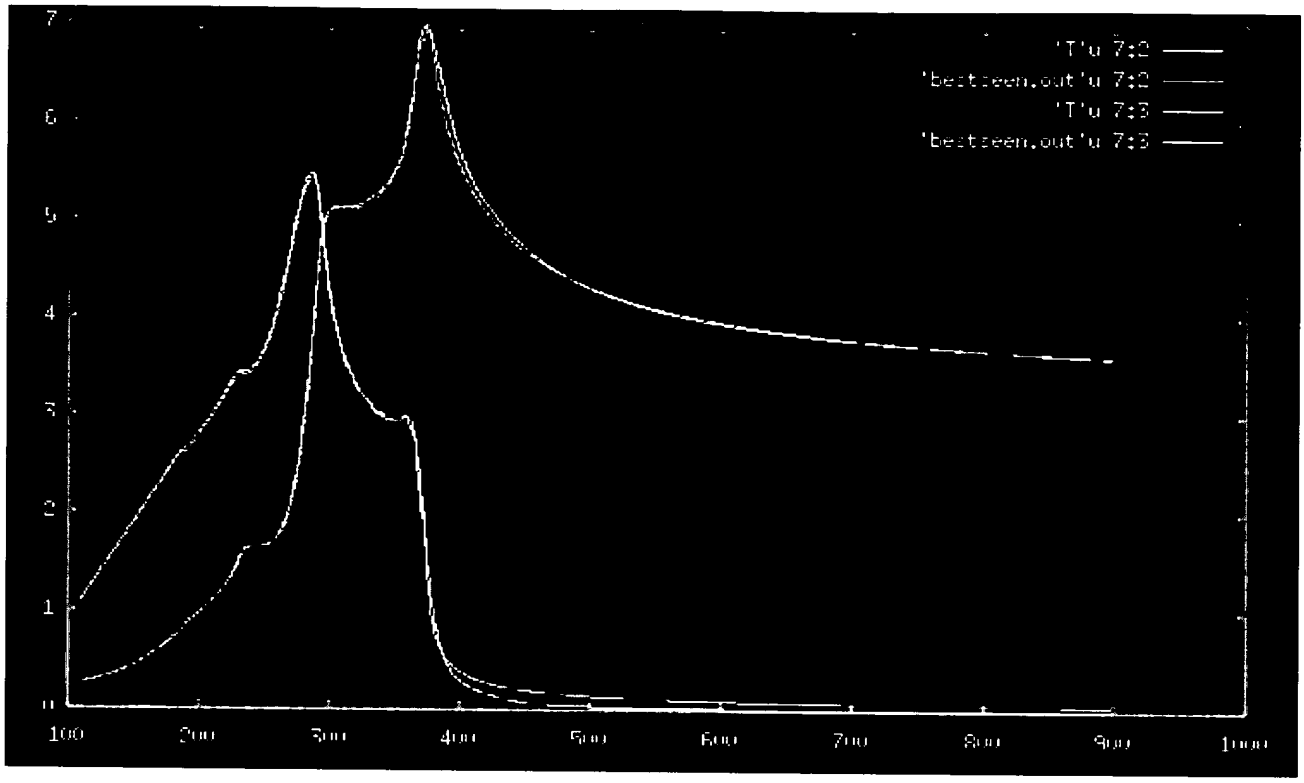

Figure 2 Refractive index n and absorption coefficient k as measured and computed by Findpoles. As can be seen the agreement is spectacular over the *entire* range.

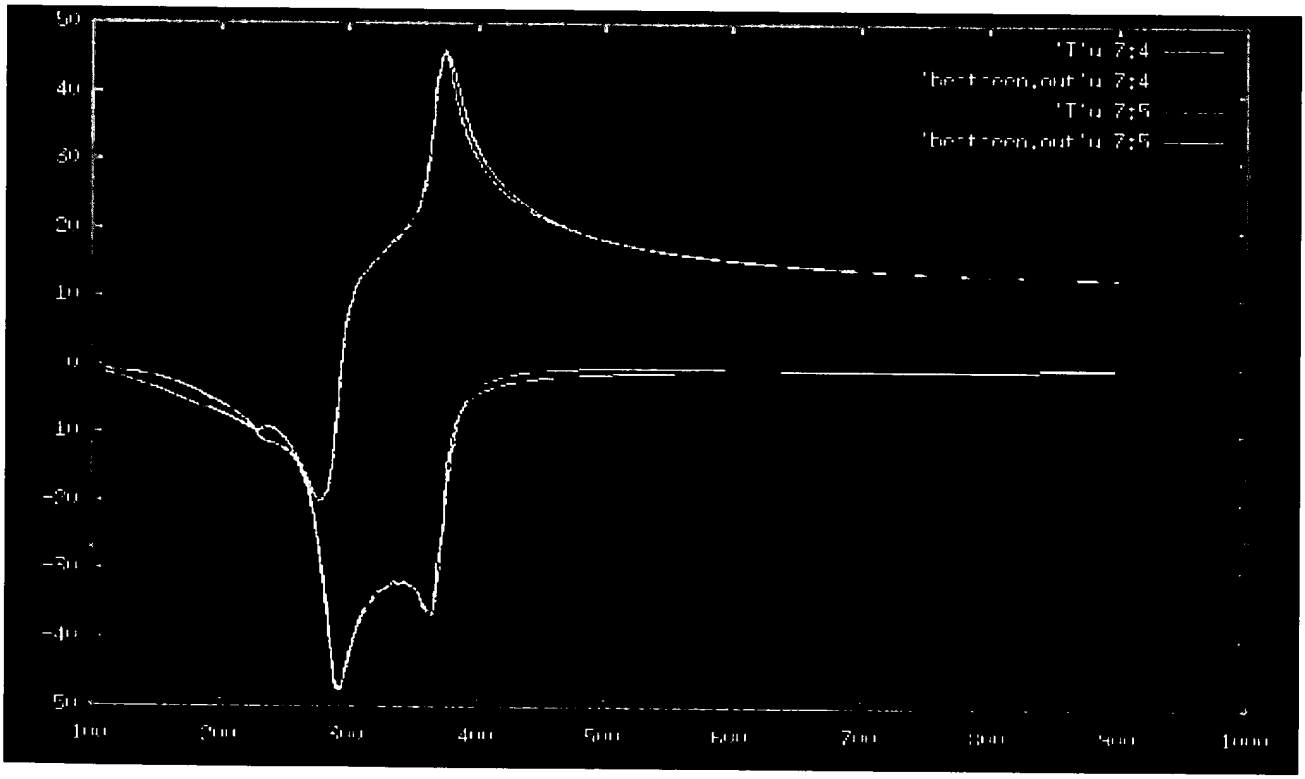

Figure 3. Real and imaginary permittivity of Silicon as measured and computed by Findpoles. As can be seen the agreement is spectacular over the *entire* range of interest.

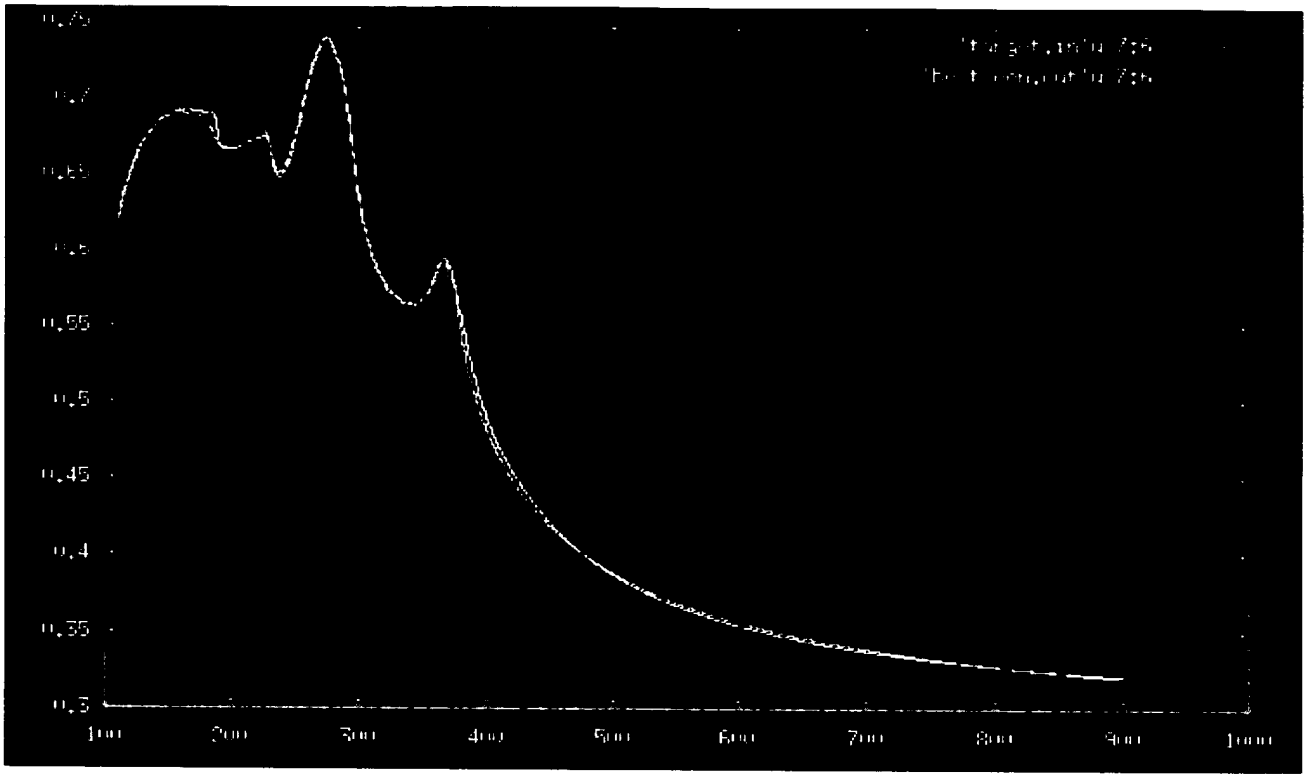

Figure 4. Calculated and measured reflection of Silicon over the entire range of interest. Agreement is very accurate as represented by the scattered wave.

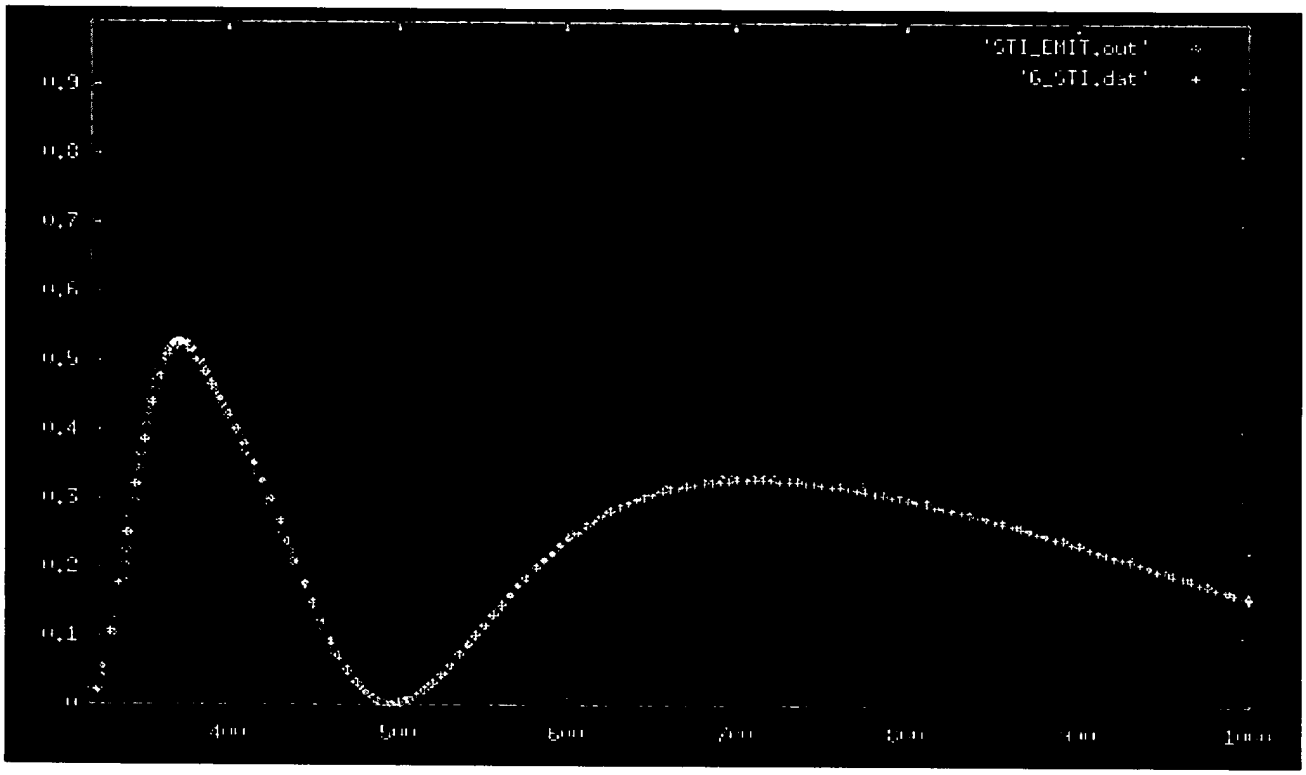

Figur 5: A comparison f th m asur d and comput d r flect d signal from a STI stack of Silicon substrat with SiO2, SiON and PolySilicon layers that f rm part f a transist r of 130nm siz .

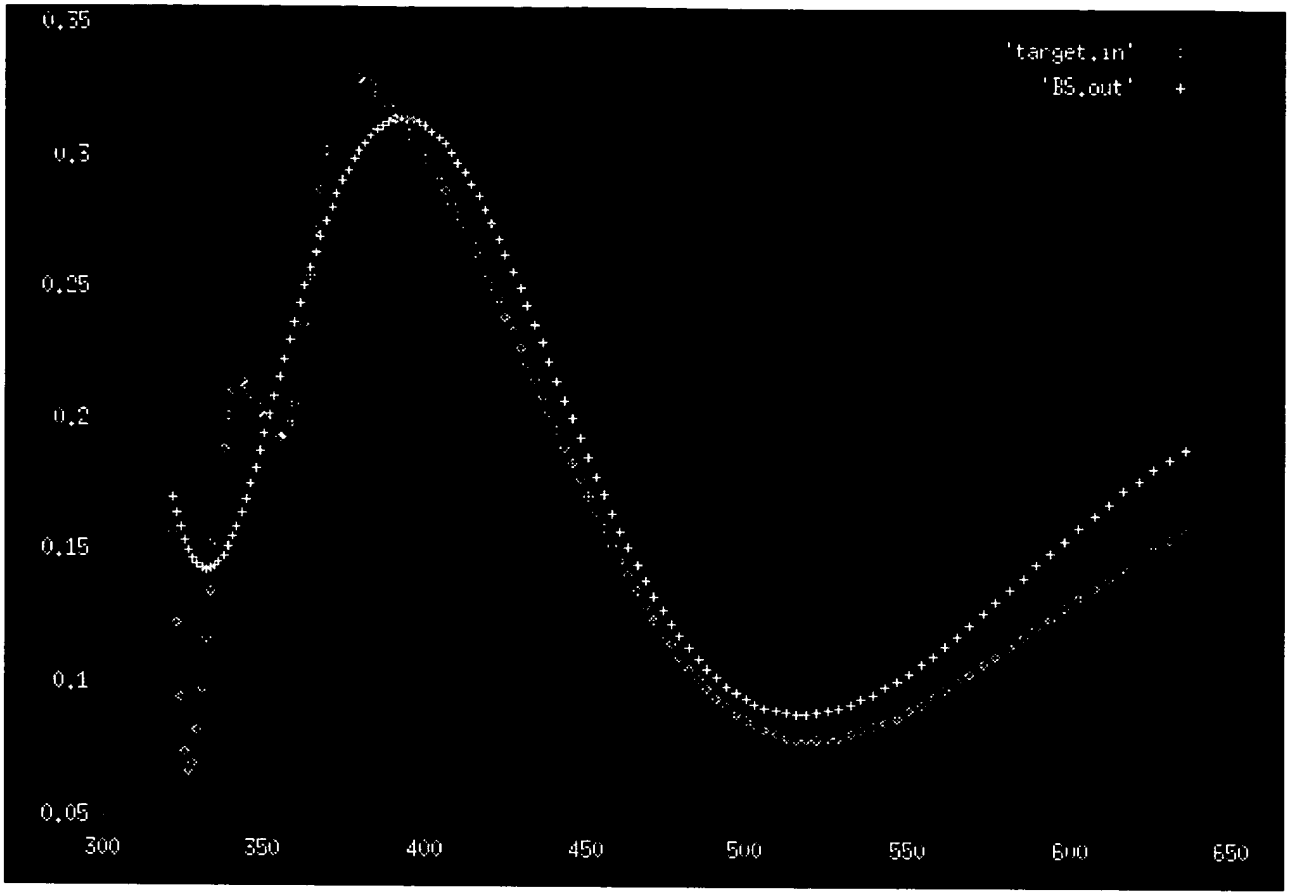

Figure 6: Comparison of measured and final calculated reflection spectra of a 300nm pitch periodic feature. The resulting reconstructed feature is identical to the SEM target.

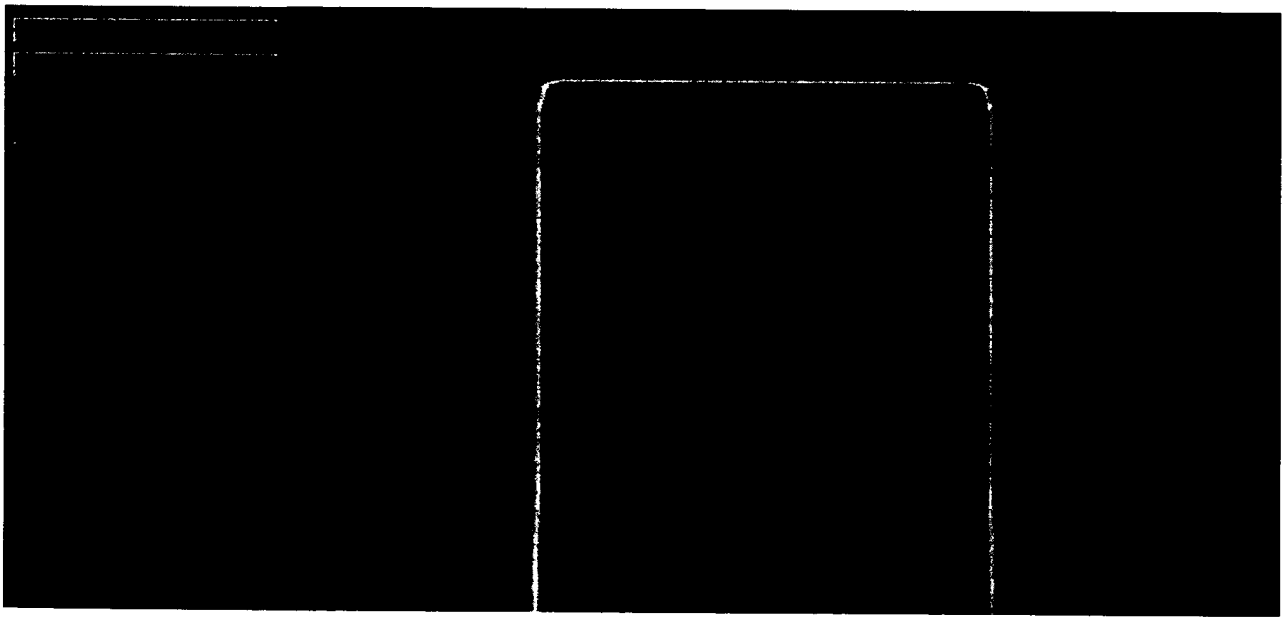

Figur 7: A r c nstructed r sist f ature of 300nm pitch L/S

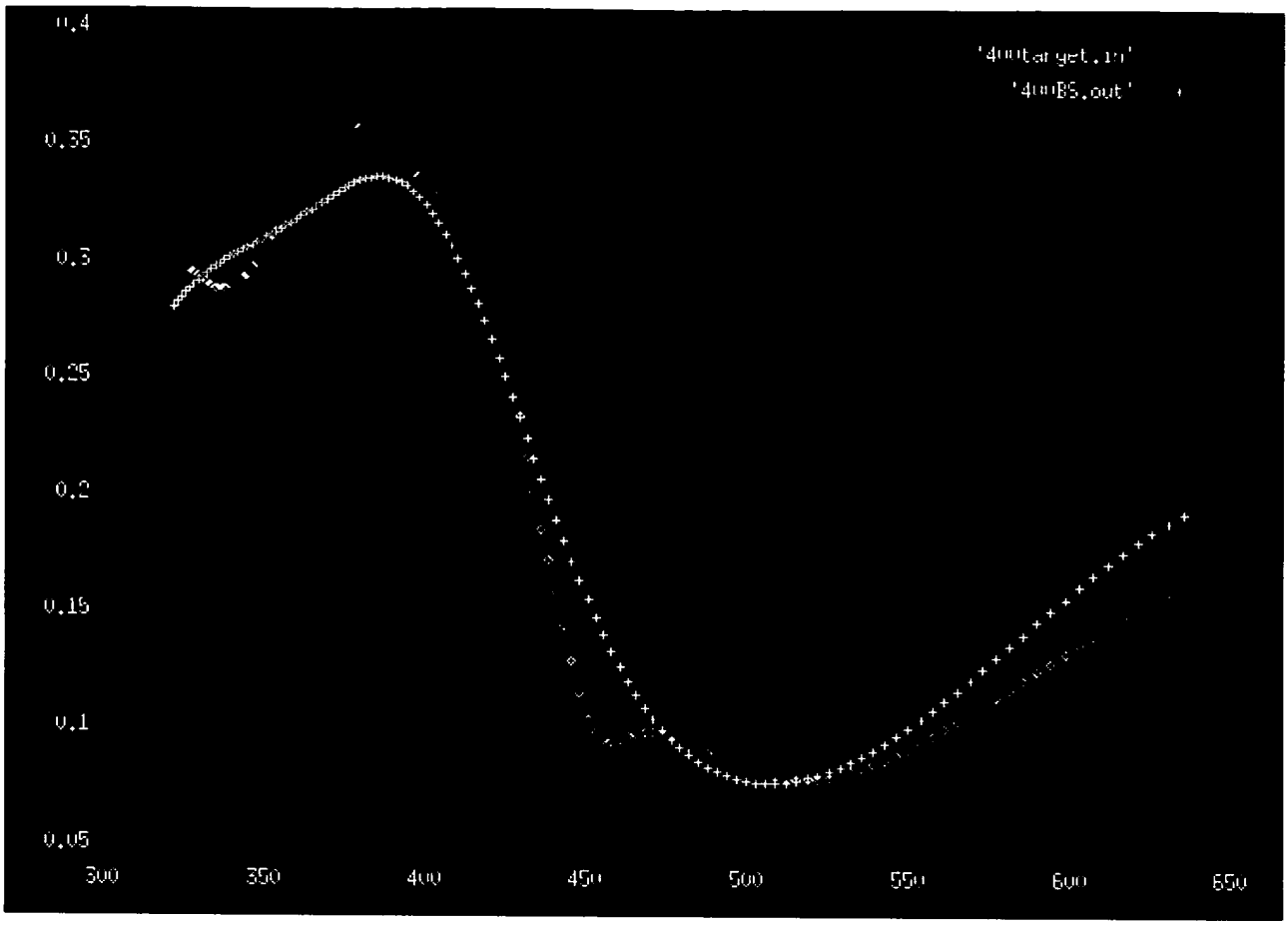

Figure 8: Comparison of measured and final calculated reflection spectra of a 400nm pitch periodic feature. The resulting reconstructed feature is identical to the SEM target.

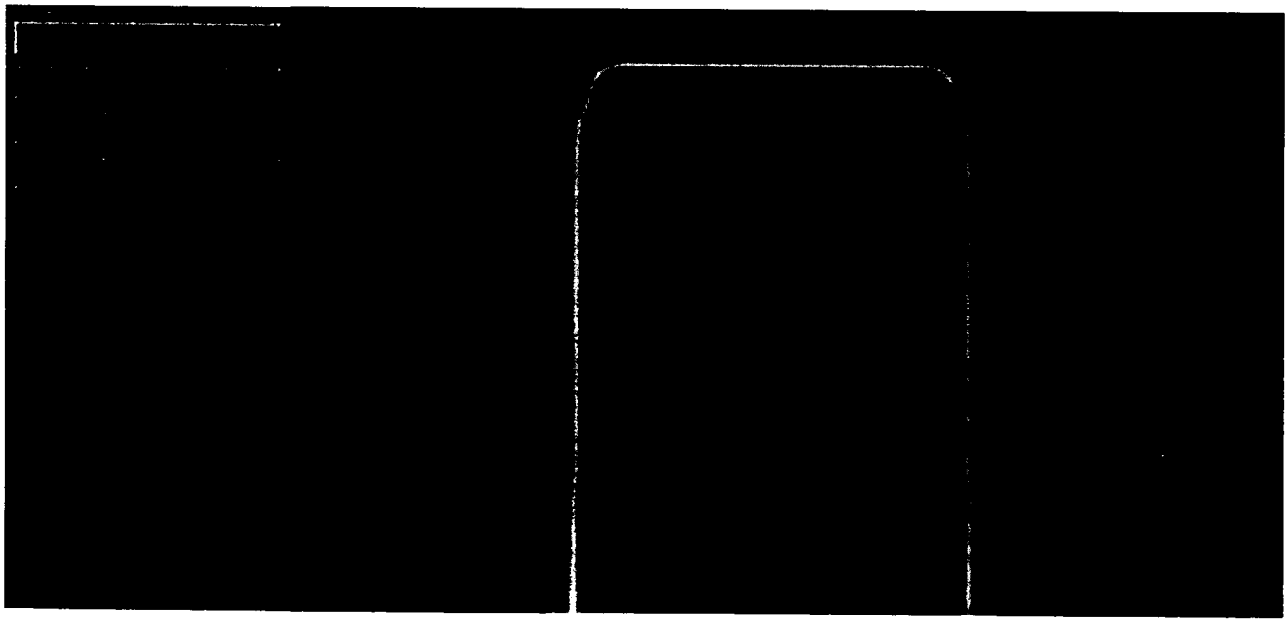

Figur 9: R construct d resist f atur of 400nm pitch L/S.

energy	n	k	real perm	imag. perm.	reflectivity	wave leng
8.28859	1.708827	0.0596079	2.91654	-0.203719	0.0689236	150
7.77055	1.662666	0.0456806	2.76237	-0.151903	0.0622138	160
7.31346	1.627461	0.0361207	2.64732	-0.11757	0.0572079	170
6.90716	1.600088	0.0293165	2.55942	-0.0938179	0.0533868	180
6.21644	1.561059	0.0205597	2.43648	-0.0641897	0.0480543	200
5.92042	1.546912	0.0176593	2.39262	-0.0546349	0.0461571	210
5.65131	1.535258	0.0153793	2.35678	-0.0472224	0.0446092	220
5.4056	1.525552	0.0135557	2.32713	-0.0413597	0.0433306	230
4.97315	1.510457	0.0108553	2.28136	-0.032793	0.0413619	250
4.78188	1.504526	0.0098394	2.2635	-0.0296074	0.0405952	260
4.60477	1.499413	0.0089838	2.24816	-0.0269407	0.0399373	270
4.44032	1.494974	0.008256	2.23488	-0.024685	0.0393685	280
4.14429	1.487689	0.0070913	2.21317	-0.0210994	0.0384399	300
4.01061	1.484678	0.0066207	2.20422	-0.0196592	0.0380579	310
3.88528	1.482006	0.0062079	2.1963	-0.0184002	0.0377197	320
3.76754	1.479622	0.0058435	2.18925	-0.0172924	0.0374188	330
3.55225	1.475566	0.0052317	2.17727	-0.0154395	0.0369082	350
3.45358	1.473832	0.0049732	2.17216	-0.0146592	0.0366906	360
3.36024	1.472262	0.0047403	2.16753	-0.013958	0.0364938	370
3.27181	1.470835	0.0045298	2.16334	-0.0133252	0.0363152	380
3.18792	1.469534	0.0043387	2.15951	-0.0127519	0.0361526	390
3.03241	1.467254	0.0040056	2.15282	-0.0117546	0.0358682	410
2.96021	1.466252	0.0038598	2.14988	-0.0113188	0.0357433	420
2.89137	1.465329	0.0037257	2.14718	-0.0109187	0.0356285	430
2.82565	1.464476	0.003602	2.14468	-0.0105501	0.0355224	440
2.7028	1.462956	0.0033817	2.14023	-0.0098946	0.0353336	460
2.64529	1.462276	0.0032833	2.13824	-0.0096021	0.0352493	470
2.59018	1.461644	0.0031916	2.13639	-0.00933	0.0351709	480
2.53732	1.461054	0.0031061	2.13467	-0.0090764	0.0350978	490
2.43782	1.459988	0.0029513	2.13156	-0.0086179	0.0349659	510
2.39094	1.459505	0.0028811	2.13015	-0.00841	0.0349061	520
2.34583	1.459052	0.0028151	2.12882	-0.0082148	0.0348501	530
2.30239	1.458626	0.002753	2.12758	-0.0080312	0.0347975	540
2.22016	1.457848	0.0026391	2.12531	-0.0076949	0.0347014	560
2.18121	1.457492	0.0025868	2.12428	-0.0075406	0.0346574	570
2.1436	1.457156	0.0025374	2.1233	-0.0073946	0.034616	580
2.10727	1.456839	0.0024904	2.12237	-0.0072563	0.0345768	590
2.03818	1.456253	0.0024036	2.12067	-0.0070005	0.0345046	610
2.0053	1.455983	0.0023633	2.11988	-0.006882	0.0344713	620
1.97347	1.455727	0.002325	2.11914	-0.0067692	0.0344398	630
1.94264	1.455484	0.0022885	2.11843	-0.0066617	0.0344098	640
1.88377	1.455032	0.0022203	2.11711	-0.0064612	0.0343542	660
1.85565	1.454822	0.0021885	2.1165	-0.0063677	0.0343283	670
1.82837	1.454621	0.002158	2.11592	-0.0062782	0.0343036	680
1.80187	1.45443	0.0021288	2.11536	-0.0061925	0.0342801	690
1.77613	1.454248	0.0021009	2.11483	-0.0061104	0.0342577	700
1.72679	1.453907	0.0020483	2.11384	-0.0059561	0.0342158	720
1.70313	1.453748	0.0020236	2.11338	-0.0058835	0.0341962	730
1.68012	1.453595	0.0019998	2.11293	-0.0058137	0.0341774	740
1.65772	1.453449	0.0019769	2.11251	-0.0057466	0.0341594	750
1.63591	1.453309	0.0019549	2.1121	-0.005682	0.0341422	760
1.59396	1.453045	0.0019132	2.11134	-0.0055599	0.0341098	780
1.57378	1.452921	0.0018935	2.11098	-0.0055021	0.0340946	790

Tabl 1: Input targ t for "Findpoles"

find poles 2.1.0b input data
1
c nduct_t rm 1
plasma_term 1
num_l rentz 5
num_Xlorentz 1
num_debye 0
420.00 84 791
nlayers 4

	min	initial	max
eps_inf	0.1000000015	0.8200767636	7.0000000000
l_sigma	0.0001000000	4.8033914566	5.0000000000
omega_pl	1.0000000000	6.5119667053	15.0000000000
alpha_pl	0.0000000000	0.9998378158	1.0000000000
S	0.1000000089	6.1372642517	9.3000001907
omega	0.4000000060	1.5478570461	7.0000000000
gamma	0.0099999998	0.0100028720	1.0000000000
S	0.0399999991	2.3346211910	4.4000000954
omega	0.4000000060	3.5085842609	13.0000000000
gamma	0.0010000000	0.0379080027	1.0000000000
S	0.0399999991	0.9923810363	4.4000000954
omega	0.4000000060	6.6716189384	12.0000000000
gamma	0.0010000000	0.2266924083	1.0000000000
S	0.0399999991	1.6832729578	4.4000000954
omega	0.4000000060	4.3492865562	9.0000000000
gamma	0.0010000000	0.0379193872	1.0000000000
S	0.0149999997	4.4830975533	8.6999998093
omega	0.8000000119	4.0481534004	8.0000000000
gamma	0.0010000000	0.0641734675	1.0000000000
XS	0.1000000089	1.8365435600	2.2999999523
Xomega	0.4000000060	5.2369093895	12.0000000000
Xgamma	0.0099999998	0.1255621761	1.0000000000
Xlambda	0.0099999998	0.6012777152	1.0000000000

Table 2: Seed input file into "Findpoles"

Matfil for input into "Fwd"
Output of "Findpol s"
l_eps_inf 0.71569538
l_sigma 8.17777292 +12
l_numlorentz 5
l_numXlor ntz 0
l_numdebye 1

deleps_p	8.52794349e-01
omega_p2	6.39123152e+31
delta_p	6.14708671e+14
deleps_p	1.57363355e+00
omega_p2	2.81803558e+31
delta_p	1.51713529e+14
deleps_p	1.68789959e+00
omega_p2	9.01482831e+31
delta_p	2.16371420e+15
deleps_p	4.39927959e+00
omega_p2	4.27885802e+31
delta_p	3.57961164e+14
deleps_p	2.52639604e+00
omega_p2	3.41288632e+31
delta_p	3.66798193e+14
delepsD_p	2.49912262e+01
tauD_p	4.95714492e-16

Table3: Output material file of "Findpoles" as input file into "Fwd"